Proceedings of the 11th International and 51st National Conference on Fluid Mechanics and Fluid Power (FMFP)
December 21-23, 2024, AMU Aligarh, Uttar Pradesh, India

FMFP2024-06-160

Drop shape estimation using Machine Learning

Aditya Kumar Singh[1], Shreya Sharma[1], Konjengbam Anand[2], and Hiranya Deka [1,*]

[1]Department of Mechanical, Materials and Aerospace Engineering, Indian Institute of Technology Dharwad, Dharwad 580007, Karnataka, India
[2] Department of Computer Science and Engineering, Indian Institute of Technology Dharwad, Dharwad 580007, Karnataka, India
* Corresponding Author, email: hdeka@iitdh.ac.in

ABSTRACT

In this study, we use a machine learning (ML) approach to predict the shape of a sessile drop based on diameter and contact angle. The train data is generated using direct numerical simulations with the help of the open-source solver Basilisk for different drop volume and contact angle values. A few ML models are tried to predict the drop shape for an arbitrary drop diameter and contact angle value. A Random Forest regression model was developed and demonstrated superior performance in predicting drop shape compared to other models. This work demonstrates an accurate method for determining drop shape using the Random Forest regression model.

Keywords: Drop, Contact Angle, Random Forest, Machine Learning

I. INTRODUCTION

A droplet resting on a solid surface is commonly known as a sessile droplet. Accurate prediction of the shape of a sessile droplet is essential in a wide range of applications, such as additive manufacturing, drop-on-demand printing, and microfluidics [1]. The shape of a droplet resting on a smooth surface depends on surface tension, contact angle, and the droplet's weight. While the air-liquid surface tension tries to make the droplet spherical to reduce the surface energy, gravity tries to flatten the droplet to minimize the potential energy. The contact angle is the angle between the tangents to the liquid-vapor interface and solid-liquid interface at the point of contact and depends on the interfacial energy of solid-liquid, solid-vapour and liquid-vapour phases. A surface is called a hydrophillic surface if the the contact angle of a water droplet is less than 90^o, and a hydrophobic surface if the contact angle of a water droplet is higher than 90^o. In this study, we use machine learning (ML) tools to predict the shape of a sessile droplet.

We have generated a comprehensive dataset on the shape of the droplet using direct numerical simulations. The volume of fluid method-based open source solver *Basilisk* [2] is used to perform the numerical simulations for different contact angles and different weights of the droplet. The resulting dataset was subsequently employed to train a ML models [3–6]. We observed that the trained model can accurately predict droplet shape based on input diameter and contact angle. Such an ML-based model significantly reduces computational costs and can accelerate the design and optimization processes in applications involving droplet dynamics.

II. METHODOLOGY

A. Direct Numerical Simulation

The direct numerical simulations are performed using the Basilisk solver to generate the dataset for drop shape for different drop volumes and contact angles. The mass and momentum conservation equations are solved in an axisymmetric (r, z) to model the flow, given as,

$$\nabla \cdot \mathbf{u} = 0, \tag{1}$$

$$\rho\left[\frac{\partial \mathbf{u}}{\partial t} + \mathbf{u}\cdot\nabla\mathbf{u}\right] = -\nabla P + \nabla\cdot\left[\mu\left(\nabla\mathbf{u} + \nabla\mathbf{u}^T\right)\right] + \sigma\kappa\hat{n}\delta_s(\mathbf{x}-\mathbf{x_f}) - \rho g\hat{e_z}, \tag{2}$$

Here, $\mathbf{u}(u, v)$ is the velocity vector where u and v stand for the components of velocity in the radial (r) and vertical (z) directions, respectively; κ is the mean curvature; $\hat{n}$ is the unit normal vectors at the interface pointing towards surrounding fluid; $\hat{e_z}$ is the unit vector in the z direction; $\delta_s(\mathbf{x} - \mathbf{x_f})$ is a delta distribution function that is zero everywhere other than at the interface where $\mathbf{x} = \mathbf{x_f}$, g the magnitude of the gravitational acceleration that acts in the negative z direction, and t is the time. The liquid and the gas are separated from each other using a volume fraction F, which is 1 for the liquid and 0 for the surrounding. The drop is initialized as a hemisphere. The advection equation for volume fraction is solved to capture the movement of the interface and the final shape of the drop.

$$\frac{\partial F}{\partial t} + \mathbf{u}\cdot\nabla F = 0. \tag{3}$$

The density, ρ, and the dynamic viscosity, μ, are calculated as a function of volume fraction F as

$$\rho = \rho_1 F + \rho_2(1-F), \tag{4}$$

$$\mu = \mu_1 F + \mu_2(1-F). \tag{5}$$

Here, ρ_1 and ρ_2 are the densities of the drop liquid and the surrounding medium, while μ_1 and μ_2 are the dynamic viscosities of the drop liquid and surrounding medium, respectively. The contact angle (θ) effect is incorporated as a boundary condition using height function.

B. Machine Learning

Machine learning (ML) has emerged as a potent tool for extracting intricate patterns from data [3, 4]. This study leverages ML to predict the geometric contour of liquid drops. By employing a suite of ML algorithms, we aim to establish a robust predictive model to predict the drop shape accurately.

The choice of machine learning algorithm is a critical step in developing an accurate and robust predictive model. In this study, four primary models were considered:

- Linear Regression: Linear regression, a foundational supervised learning technique, seeks to establish a linear relationship between input features (contact angle and diameter) and the target variable (drop geometry). This method assumes a linear correlation between the predictors and the dependent variable. Model coefficients are determined by minimizing the residual sum of squares. In comparison, simple and interpretable linear regression might be limited in capturing complex, nonlinear relationships inherent in droplet formation.
- Gradient Boosting: Gradient boosting is an iterative ensemble method that builds models to improve predictive accuracy sequentially. Each subsequent model focuses on correcting errors made by previous models. This approach often yields high performance but can be computationally intensive.
- Decision Tree: Decision trees represent a hierarchical structure where internal nodes correspond to feature-based decisions, and leaf nodes represent predicted drop geometries. This model partitions the feature space into distinct regions, assigning a specific geometry to each region. While interpretable, decision trees can be susceptible to overfitting, especially when dealing with noisy or high-dimensional data.
- Random Forest: Random Forest is an ensemble method that constructs multiple decision trees during training. Each tree independently predicts the drop geometry based on a random subset of the data. The final prediction is an aggregate of these individual predictions. This approach is adept at handling non-linearity and interactions among features, making it suitable for complex systems like droplet formation.

The dataset of the shape of the droplet is generated using the direct numerical simulation for different drop diameters and contact angles. Robust model training was ensured by the dataset's variability, which covered a broad range of contact angles and drop sizes. Every data point comprised precise geometric details (r and z coordinates of the interface) about the droplet, including volume.

From the raw dataset, relevant characteristics were taken out to prepare the data for training machine learning models. Essential characteristics comprised: a) contact angle, b) drop diameter, c) (r, z) coordinates of the interface

The preprocessing procedures listed below were used to enhance model stability and performance:

- Outlier Detection and Removal: We found and eliminated extreme data points that can have a negative impact on model training.
- Data Splitting: To thoroughly evaluate model performance, the dataset was split into training, validation, and testing sets.

The selected ML models (linear regression, gradient boosting, decision tree, and random forest) were implemented using ML libraries, e.g., Scikit-learn[7]. Standard measures were used to evaluate the model's performance. The cross-validation with DNS data is performed to appraise the generalization capacity and performance of various models. The best-performing model was chosen for further analysis and possible implementation based on the evaluation criteria and visual inspection.

C. Validation

The Basilisk solver has been extensively used by several researchers to model the droplet dynamics. We redirect readers to Ref. [8] for the contact angle model used in the solver and the validation of the solver. Further details about the solver and validations are available in Refs. [9–11].

III. RESULTS AND DISCUSSION

The direct numerical simulations are initialized with a hemispherical drop resting on a surface. The diameter of the hemisphere can be calculated by equating the volume to a spherical drop of certain diameter. In the absence of gravity the shape of the drop depends only on the contact angle (and surface tension which we kept constant in all the simulations). The gravitational force try to flatten the droplet to minimize the potential energy and is more prominent for larger drops. The shape of three drops of diameter 2 mm, 5 mm and 10 mm, all having 90^o contact angle are shown in Fig. 1. Indeed the shape of the drop depends on the value of Bond number (Bo) which is the ratio of gravitational force to surface tension force and is defined as $Bo = \Delta\rho g D^2/\sigma$. We generated a comprehensive dataset for different values of Bo and for different θ.

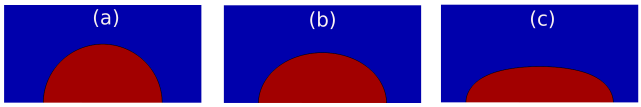

Figure 1: **The shape of a droplets of (a)** D **= 2 mm, (b)** d **= 5 mm and (c)** D **= 10 mm are plotted. The contact angle in all the cases is** $\theta = 90°$**.**

Next, we use this dataset to train the ML models. As mentioned in Sec. II-B, we trained four different models to predict the shape of a droplet with the input parameters of Bo and θ. A comparison of the predicted drop shape for a 5.5 mm diameter droplet for contact angle $\theta = 75°$ of each model and the DNS result are shown in Figs. [2-5]. It is evident that the Random Forest model gives the closest match with the DNS results. We have calculated the error involved with each model to optimize the choice of the

models quantitatively. The error is calculated as

$$\text{Error} = \frac{1}{n}\sum\left|\frac{z_s - z_p}{z_s}\right| \times 100\%, \tag{6}$$

where z_s and z_p are the z-coordinates of the drop interface at same radial (r) location obtained from DNS and ML prediction respectively, and n is the total number of coordinate points considered. A comparison of the error involved with each predictive model is presented in Table 1. It is evident in Table 1 that out of the four models, the Random Forest performs better than the other three models. The Random Forest model is computationally less expensive and, because of its superior accuracy, can be designated as the most effective model. Here, we considered 114 datasets for training the ML algorithm. The accuracy can be improved with a large number of training datasets.

Figure 2: **The shape of a droplet (a) obtained from DNS and (b) predicted from Linear Regression Model.**

Figure 3: **The shape of a droplet (a) obtained from DNS and (b) predicted from Gradient Boosting Model.**

Figure 4: **The shape of a droplet (a) obtained from DNS and (b) predicted from Decision tree Model.**

Figure 5: **The shape of a droplet (a) obtained from DNS and (b) predicted from Random Forest Model.**

A comparison of the predicted drop shape and the DNS results is shown in Figs. [6-17]. Figs [6-8] show the comparison for a 2 mm diameter droplet for contact angle $\theta = 45°$ (Fig. [6]), $\theta = 90°$ (Fig. [7]), and $\theta = 135°$ (Fig. [8]) which shows a good match between the DNS and ML predicted results. Figs [9-11] show the comparison for a 4 mm diameter droplet for contact angle $\theta = 45°$ (Fig. [9]), $\theta = 90°$ (Fig. [10]), and $\theta = 135°$ (Fig. [11]). Figs [12-14] show the comparison for a 6 mm diameter droplet for contact angle $\theta = 45°$ (Fig. [12]), $\theta = 90°$ (Fig. [13]), and $\theta = 135°$ (Fig. [14]). Figs [15-17] show the comparison for a 2.4 mm diameter droplet for contact angle $\theta = 75°$ (Fig. [15]), $\theta = 90°$ (Fig. [16]), and $\theta = 120°$ (Fig. [17]). The good consistency between the DNS and ML predicted results corroborates the prediction ability of the ML model. The ML model offers a significant computational advantage over traditional simulation methods, proving valuable information for optimizing droplet-based systems. Future work should consider including additional physical parameters and exploring deep learning techniques to improve accuracy further.

Table 1: **A comparison of the error involved with each predictive model is presented for a 5 mm diameter droplet with $\theta = 75^0$.**

Model	**Error (%)**
Linear Regression	137.96
Gradient Boosting	92.26
Decision Tree	10.67
Random Forest	9.73

Figure 6: **The shape of a droplet (a) obtained from DNS and (b) predicted from ML are plotted for D = 2 mm and $\theta = 45°$.**

Figure 7: **The shape of a droplet (a) obtained from DNS and (b) predicted from ML are plotted for D = 2 mm and $\theta = 90°$.**

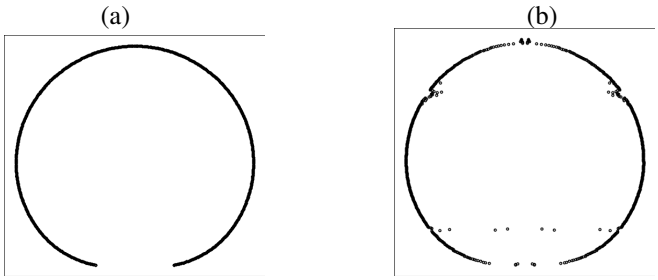

Figure 8: **The shape of a droplet (a)obtained from DNS and (b) predicted from ML are plotted for D = 2 mm and $\theta = 135°$.**

Figure 9: **The shape of a droplet (a) obtained from DNS and (b) predicted from ML are plotted for D = 4 mm and $\theta = 45°$.**

Figure 10: **The shape of a droplet (a) obtained from DNS and (b) predicted from ML are plotted for D = 4 mm and $\theta = 90°$.**

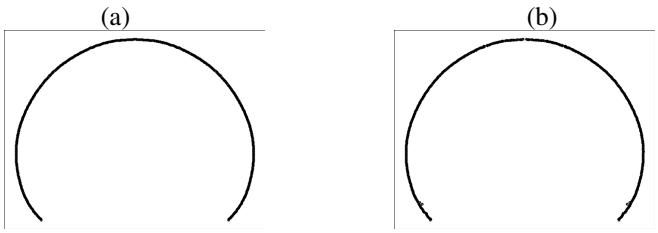

Figure 11: **The shape of a droplet (a) obtained from DNS and (b) predicted from ML are plotted for D = 4 mm and $\theta = 135°$.**

Figure 12: **The shape of a droplet (a) obtained from DNS and (b) predicted from ML are plotted for D = 6 mm and $\theta = 45°$.**

Figure 13: **The shape of a droplet (a) obtained from DNS and (b) predicted from ML are plotted for D = 6 mm and $\theta = 90°$.**

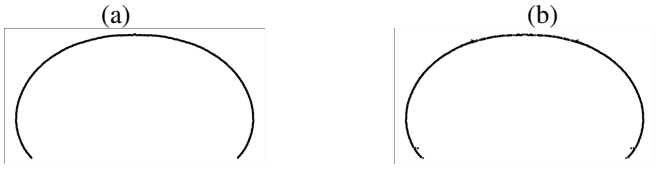

Figure 14: **The shape of a droplet (a) obtained from DNS and (b) predicted from ML are plotted for D = 6 mm and $\theta = 135°$.**

Figure 15: **The shape of a droplet (a) obtained from DNS and (b) predicted from ML are plotted for D = 2.4 mm and $\theta = 75°$.**

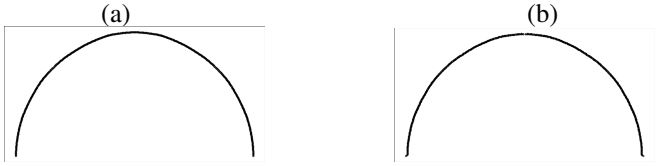

Figure 16: **The shape of a droplet (a) obtained from DNS and (b) predicted from ML are plotted for D = 2.4 mm and $\theta = 90°$.**

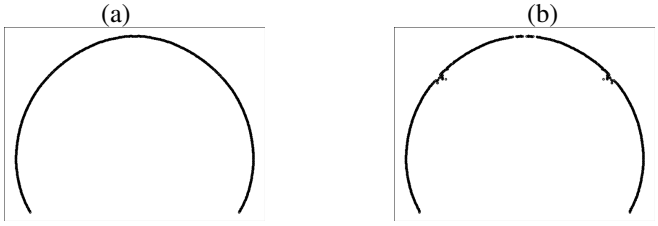

Figure 17: **The shape of a droplet (a) obtained from DNS and (b) predicted from ML are plotted for D = 2.4 mm and $\theta = 120°$.**

IV. CONCLUSIONS

In this study, we have developed a machine learning model capable of predicting shape of a sessile depending on its diameter and contact angle. The training dataset is

generated using the direct numerical simulations. Four ML models have been tested to predict the shape of a sessile droplet: Linear Regression model, Gradient Boost model, Decision Tree model, and Random Forest model. The Random Forest Regression model demonstrated superior performance, achieving least error in predicting droplet geometry. ML model offers a significant reduction in computational costs compared to traditional simulation-based approaches, making it a valuable tool for accelerating the design and optimization of droplet-based applications.

ACKNOWLEDGEMENTS

Hiranya Deka acknowledges the financial support from the Indo-French Centre for the Promotion of Advanced Research (IFCPAR/CEFIPRA) through Project no. 70T10-1.

NOMENCLATURE

Bo	Bond Number	–
F	Volume Fraction	–
κ	mean curvature	m^{-1}
μ	dynamic viscosity	$N \cdot s/m^2$
ρ	density	kg/m^3
r	Radius of drop	mm
θ	Contact Angle	$^\circ$
$\mathbf{u}$ (u,v)	velocity vector	m/s
$\hat{e_z}$	unit vector in the z direction	–

REFERENCES

[1] Angshuman Kapil, Vatsalya Sharma, Jan De Pauw, and Abhay Sharma. Exploring impact, spreading, and bonding dynamics in molten metal deposition for novel drop-on-demand printing. *Materials & Design*, 238:112633, 2024.

[2] Basilisk. http://basilisk.fr.

[3] Jerome Friedman. The elements of statistical learning: Data mining, inference, and prediction. *(No Title)*, 2009.

[4] Christopher M Bishop and Nasser M Nasrabadi. *Pattern recognition and machine learning*, volume 4. Springer, 2006.

[5] Leo Breiman. Random forests. *Machine learning*, 45:5–32, 2001.

[6] Jerome H Friedman. Greedy function approximation: a gradient boosting machine. *Annals of statistics*, pages 1189–1232, 2001.

[7] Fabian Pedregosa, Gaël Varoquaux, Alexandre Gramfort, Vincent Michel, Bertrand Thirion, Olivier Grisel, Mathieu Blondel, Peter Prettenhofer, Ron Weiss, Vincent Dubourg, et al. Scikit-learn: Machine learning in python. *the Journal of machine Learning research*, 12:2825–2830, 2011.

[8] S. Afkhami, S. Zaleski, and M. Bussmann. A mesh-dependent model for applying dynamic contact angles to vof simulations. *Journal of Computational Physics*, 228(15):5370–5389, 2009.

[9] Stéphane Popinet. Gerris: a tree-based adaptive solver for the incompressible euler equations in complex geometries. *Journal of Computational Physics*, 190(2):572–600, 2003.

[10] Stéphane Popinet. An accurate adaptive solver for surface-tension-driven interfacial flows. *Journal of Computational Physics*, 228(16):5838–5866, 2009.

[11] Hiranya Deka, Gautam Biswas, Kirti Chandra Sahu, Yash Kulkarni, and Amaresh Dalal. Coalescence dynamics of a compound drop on a deep liquid pool. *Journal of Fluid Mechanics*, 866:R2, 2019.